INSTITUTE OF PHYSICS - SRI LANKA

Phase space studies of complex Henon Heiles potentials

A. Nanayakkara[a*] and C. Abayaratne[b]

[a]*Institute of Fundamental Studies, Hanthana Road, Kandy, Sri Lanka.*

[b]*Department of Physics, University of Sri Jayawardenepura, Nugegoda, Sri Lanka.*

Abstract

PT symmetric 2-D Henon-Heiles Potentials are studied semiclassically. We generalize the definition of Poincare' surface of sections to identify both regular and chaotic motion in the complex phase space. Definition of Lyapunov exponents is extended for complex trajectories. Both regular and chaotic trajectories are identified for the complex *PT* symmetric potentials using the new definition of Lyapunov exponents. A new quantization condition is introduced and its applicability to complex phase space is discussed.

1. INTRODUCTION

Henon Heiles potential [1] in two dimensions $V = \frac{1}{2}\left(\omega^2{}_x x^2 + \omega^2{}_y y^2\right) + \lambda x(y^2 + \eta x^2)$, for real parameters λ and η has received considerable attention during the last few decades from various branches of physics and astronomy due to its applicability in studying the motion of stars in the galaxy, molecular vibrations, and the chaotic behavior of Hamiltonian systems. The above system is dynamically nonseparable and quasiperiodic. The phase space of this potential consists of both regular, chaotic, and mixed regions. The energy spectrum of this potential has been studied using both semicalssical and quantum mechanical methods [2]. Most of the semiclassical methods are applicable when the motion is periodic or qasiperiodic. Two of the semiclassical methods that have been successfully applied to obtain eigen energies of the above

* Coprresponding author (E-mail: asiri@ifs.ac.lk)

potential are based on EBK quantization rule using integration along invariant curves on Poincare surfaces and caustics.

Quite recently, quantum mechanical *PT* symmetric theories associated with the complex Henon Heiles potential has been investigated by Bender et al. [3]. Such theories seem to possess real and positive spectra. They have obtained the low lying quantum energy levels using higher order perturbation theory.

In this paper we report the results obtained by a semiclassical study of the complex *PT* symmetric potential

$$V_1 = \frac{1}{2}\left(\omega^2{}_x x^2 + \omega^2{}_y y^2\right) + i\lambda x(y^2 + \eta\, x^2)\,, \qquad (1)$$

and the real potential

$$V_2 = \frac{1}{2}\left(\omega^2{}_x x^2 + \omega^2{}_y y^2\right) + \lambda x(y^2 + \eta\, x^2)\,. \qquad (2)$$

where λ and η are real parameters.

The potential in (2) is studied for comparison purposes. The outline of the paper is as follows. In section 2, first we study the semiclassical trajectories using Poincare surfaces of sections for the real potential V_2 in both real and complex phase spaces. Then the complex potential V_1 is studied in a similar manner. In section 3, we study the complex potential V_1 semiclassically. In addition, Lyapunov exponents are calculated to study the trajectories where Poincare surfaces contain only a very few points in the chaotic energy region. For comparison purposes, Lyapunov exponents are also calculated for trajectories obtained under the real potential V_2. In section 4, semiclassical quantization methods are discussed for complex potentials.

2. CLASSICAL PHASE SPACE FOR REAL POTENTIALS

In this section, we study both the real and the complex phase spaces of the real 2-D Henon Heiles potential. Traditionally, phase space studies are carried out in real space. However, in the case of a complex potential, even with a purely real starting point, the subsequent trajectory will consist of complex phase space points arising due to the complex potential. With the goal of treating such cases in mind, we extended the traditional real phase space to complex phase space by generalizing the coordinates and momenta as complex quantities. Complex phase space inevitably introduces complex momenta in the subsequent motion even under the influence of a purely real potential. For these reasons it would be interesting to study a real potential in complex phase space as well.

The concept of surface of section introduced by Poincare many years ago has been employed to study the chaotic behavior of dynamical systems by many authors for real potentials [4]. Now we extend the concept of Poincare surface of section to the complex plane to study chaos in complex phase space.

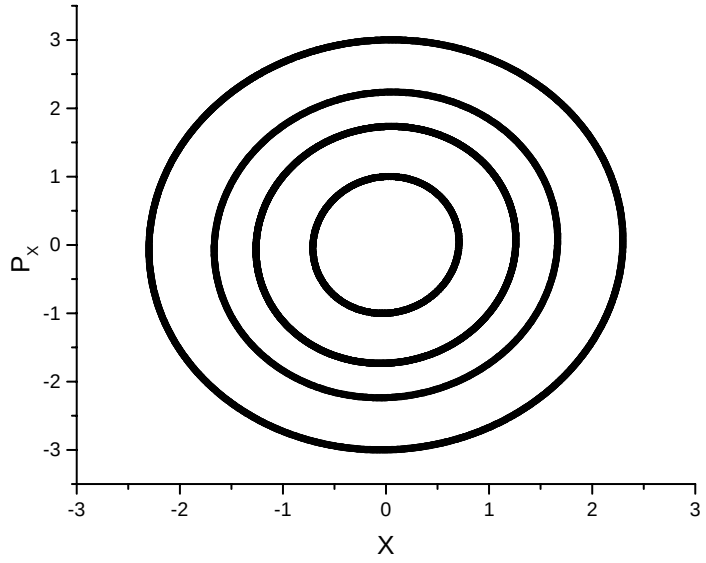

Fig. 1 Example of a Poincare surface of section at $y = 0$ for four trajectories of the real potential V_2, all with the same energy $E = 5.0$, but different initial conditions.

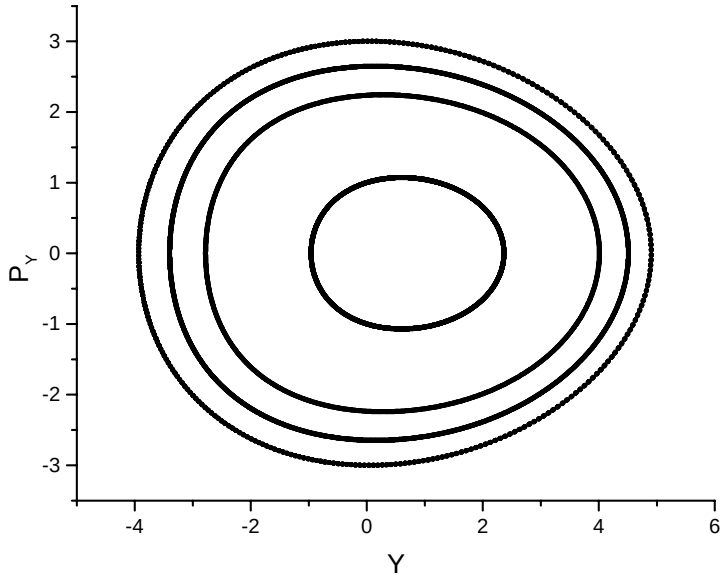

Fig. 2 Example of a Poincare surface of section at $x = 0$ for the four trajectories in Fig. 1, all with the same energy $E = 5.0$, but different initial conditions.

Real Poincare surfaces for 2-D potentials are usually obtained by solving Hamilton's equations of motion numerically and collecting the points (x, P_x) when $y = 0$ and (y, P_y) when $x = 0$. By observing the patterns so obtained, it is possible to identify whether the behavior of a certain system is largely quasi-periodic or largely ergodic. The Hamiltonian for the potential V_2 is

$$H(x, p_x, y, p_y) = \frac{1}{2}\left(p^2{}_x + p^2{}_y\right) + \frac{1}{2}\left(\omega^2{}_x x^2 + \omega^2{}_y y^2\right) + \lambda x(y^2 + \eta\, x^2) \qquad (3)$$

In this study we solve Hamilton's equations of motion using the above Hamiltonian for $\omega_x = 0.7$, $\omega_y = 1.3$, $\lambda = -0.1$, and $\eta = 0.1$ with the initial conditions $x = 0$, $y = 0$ and obtain Poincare surfaces for both quasiperiodic and chaotic energies. Figures (1) and (2) represent a part of the phase space where the motion is quasiperiodic. For the real potential V_2 with parameters $\omega_x = 0.7$, $\omega_y = 1.3$, $\lambda = -0.1$, and $\eta = 0.1$, Poincare surfaces look similar to figures 1 and 2 for all energies $E < 10.0$ and the motion is quasiperiodic. For quasiperiodic motion, studied using Poincare surfaces, semiclassical energies can be calculated by the EBK quantization method as described by Noid and Macus [4] . We will discuss this in the next section.

In figures (3) and (4), the motion corresponding to mixed regions is shown. Two of the trajectories are chaotic while the other two are quasiperiodic. If the energy is increased further, all the trajectories would become completely chaotic. Now let us study the same potential in complex phase space to see how the Poincare surfaces look for both the quasiperiodic and the ergodic energies. In order to obtain Poincare surfaces in complex phase space, we solve Hamilton's equations of motion in the complex plane. As in the real case, we collect the points (x, P_x) when $y = 0$ and (y, P_y) when $x = 0$. However, x, y, P_x, and P_y are now complex quantities, and it is possible to identify quasi-periodic and ergodic regions by observing various combinations of the real and imaginary projections of them.

For the real potential in (1), in order to obtain Poincare surfaces in complex phase space, we introduced small complex quantities to the initial values of x, y, P_x, and P_y. As a result, all points on the trajectory lie in the complex plane. Figures 5- 8 show Poincare surfaces when the system is quasiperiodic while Figures 9-12 are illustrations of ergodic motion of the system. Figures 5,6 and 9,10 look quite similar to those obtained for real phase space. It is also found in this study that in both real and complex motions, transitions from quasi-periodic to chaotic take place at the same energies. This is an indication that, in general, for a real potential, both the real and the real part of the complex trajectories behave alike. Figures (7) and (8) show the projections of the Poincare surface of sections on the complex coordinate planes of x and y for a quasiperiodic trajectory. In a recent, paper [5], it was shown how to obtain quantum eigen energies numerically using contours in the complex phase space for 1-D motion. It is interesting to find out how to extend the ideas in [5] for 2-D motion using contours like those in figures (7) and (8). This will be discussed in section 4.

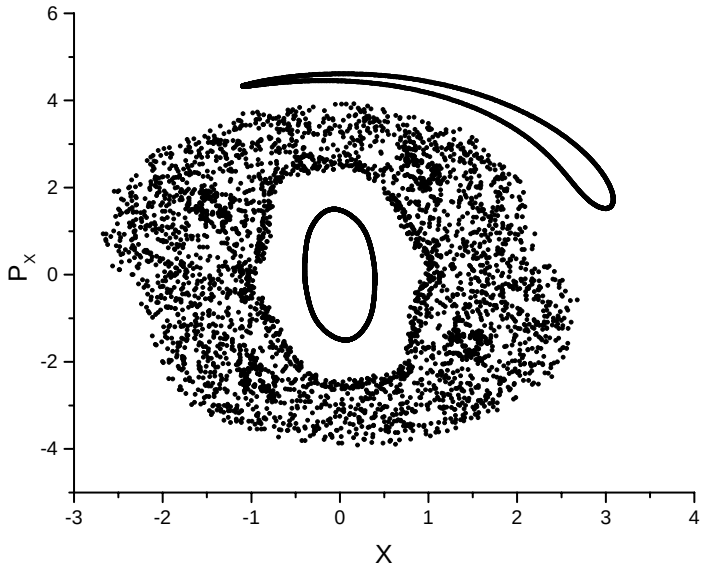

Fig. 3. Example of a Poincare surface of section at $y = 0$ for the five trajectories of the real potential V_2, all with the same energy $E = 11.0$, but different initial conditions.

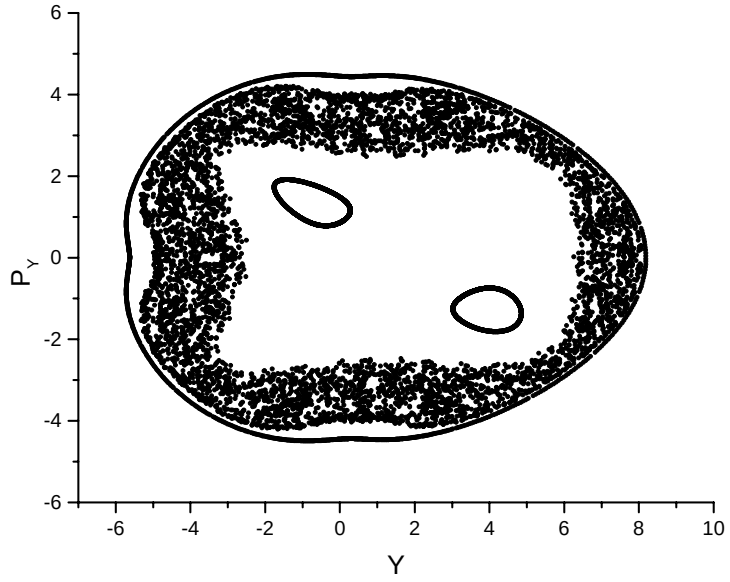

Fig. 4. Example of a Poincare surface of section at $y = 0$ for the five trajectories, all with the same energy $E = 11.0$, but different initial conditions.

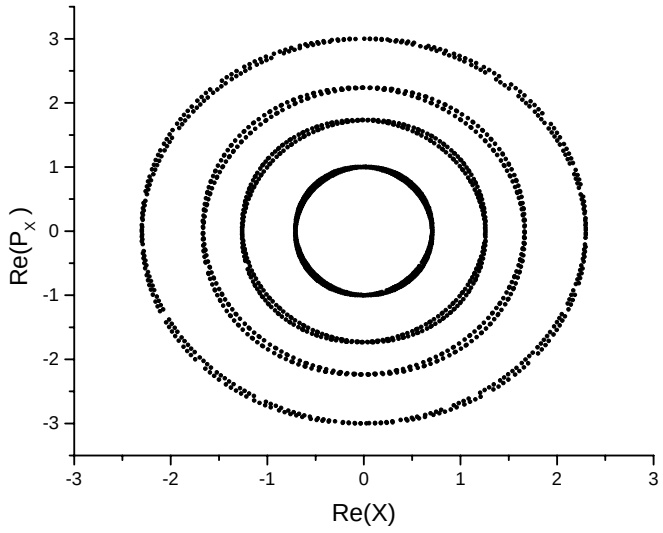

Fig. 5. Example of a Poincare surface of section at $y = 0$ for the four trajectories of the real potential V_2 in complex phase space, all with the same energy $E = 5.0$, but different initial conditions. Only the real projections of the coordinate x and momentum P_x are shown here.

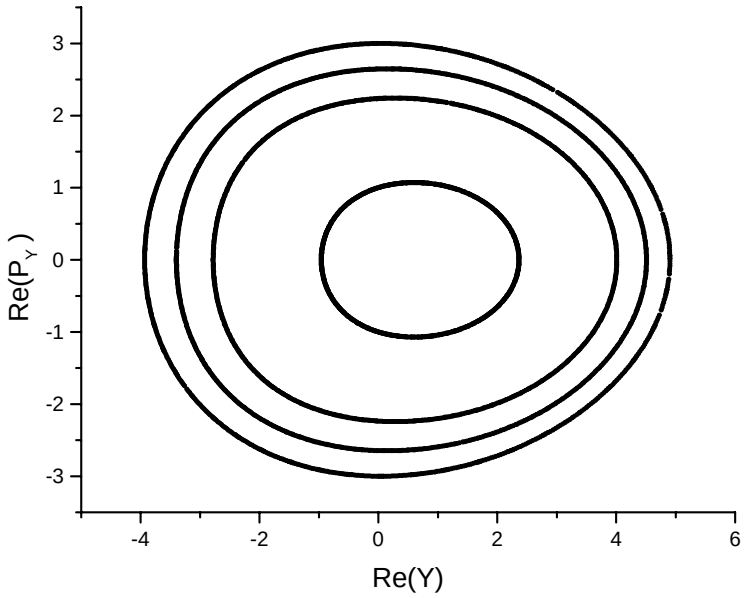

Fig. 6. Example of a Poincare surface of section at $x = 0$ for the four trajectories of the real potential V_2 in complex phase space, all with the same energy $E = 5.0$, but different initial conditions. Only the real projections of the coordinate y and momentum P_y are shown here.

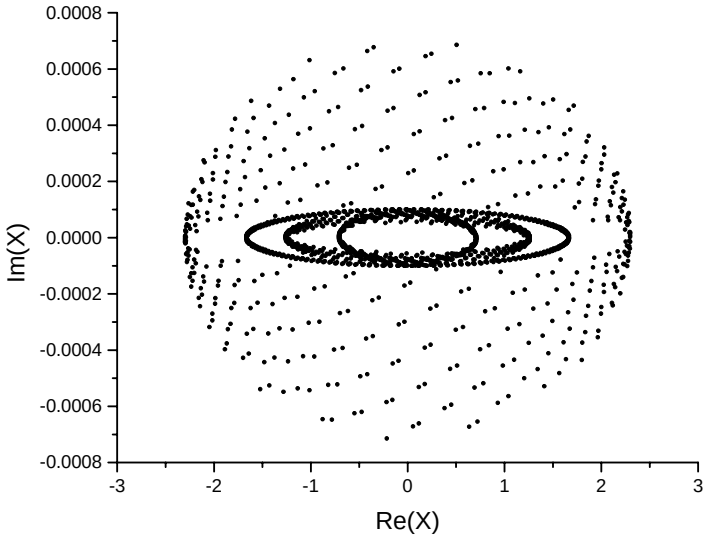

Fig. 7. Same as Figure 5, but only the projections of the Poincare surface of sections on the complex coordinate plane of x are shown here.

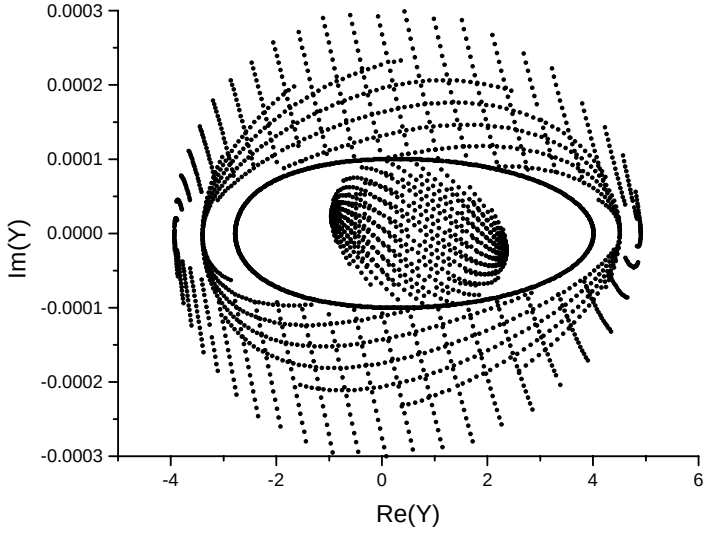

Fig. 8. Same as Figure 6, but only the projections of the Poincare surface of sections on the complex coordinate plane of y are shown here.

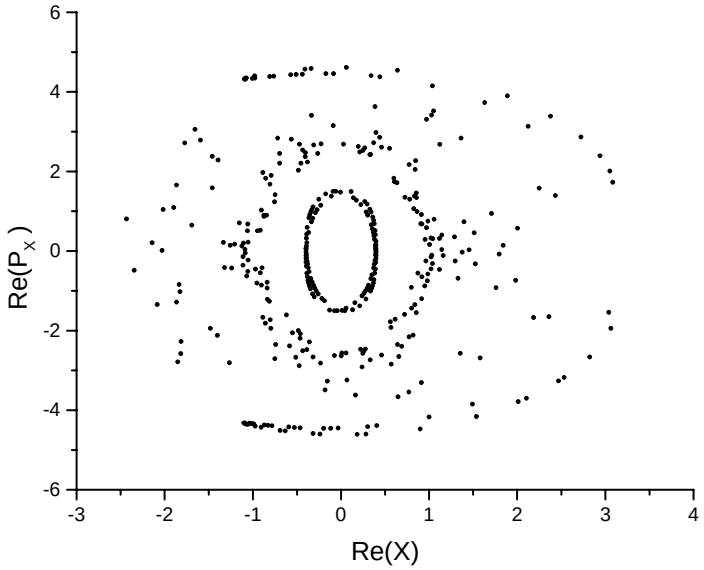

Fig. 9. Example of a Poincare surface of section at $y = 0$ for the four trajectories of the real potential V_2 in complex phase space, all with the same energy $E = 11.0$, but different initial conditions. Only the real projections of the coordinate x and momentum P_x are shown here.

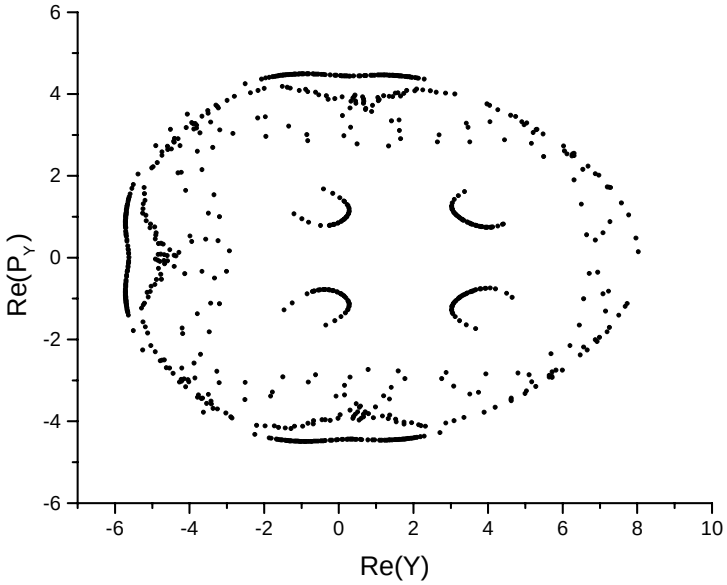

Fig. 10. Example of a Poincare surface of section at $x = 0$ for the four trajectories of the real potential V_2 in complex phase space, all with the same energy $E = 11.0$, but different initial conditions. Only the real projections of the coordinate y and momentum P_y are shown here.

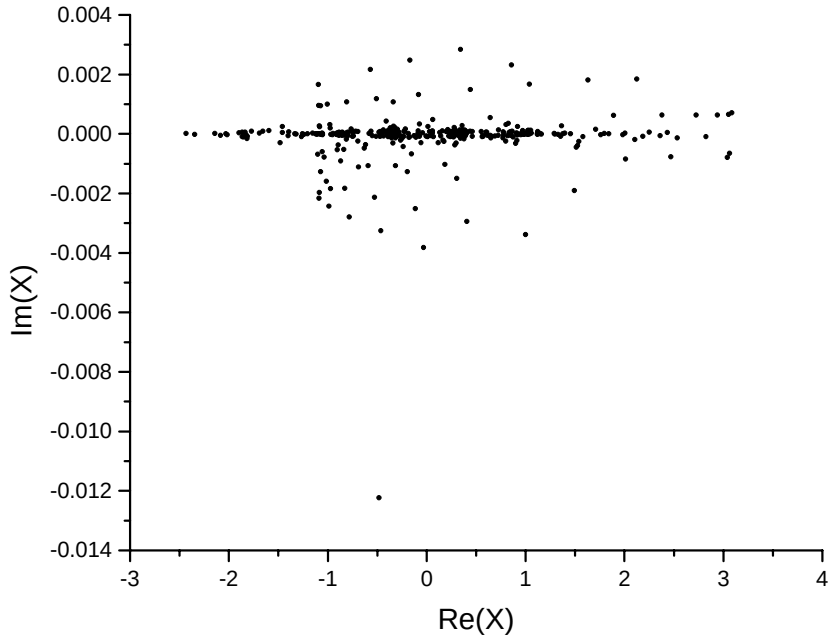

Fig. 11. Same as Figure 9. but only the projections of the Poincare surface of sections on the complex coordinate plane of x are shown here.

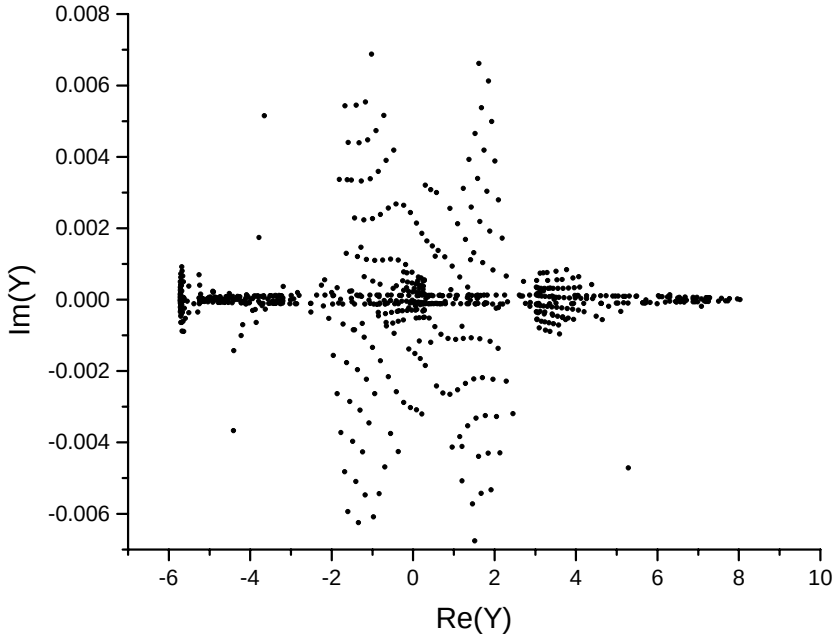

Fig. 12. Same as Figure 10, but only the projections of the Poincare surface of sections on the complex coordinate plane of y are shown here.

3. CLASSICAL PHASE SPACE FOR COMPLEX POTENTIALS

In this section, we study the quasiperiodic and ergodic nature of the phase space of the complex potential V_1. In the last section, we saw how the projections of Poincare surfaces change when the system makes a transition from the quasiperiodic region to the ergodic region. Here we attempt to identify changes that occur in such transitions when the potential is complex. Although, for the real phase space of a real potential, quasiperiodicity and ergodicity are based on the existence of invariant tori, it is not very clear what analogues to the invariant tori exist in complex phase space. However, the complex phase space for a 2-D complex potential may be considered as a subspace of a real phase space of a 4-D real potential. Further studies have to be carried out to get a clearer picture. In this study, we used the Lyapunov exponents as a measure of chaos for both real and complex potentials.

The 1-D Lyapunov exponent [6] for both real and complex classical motion is given by,

$$L_e = \lim_{\substack{t\to\infty \\ d(0)\to 0}} \frac{1}{t} \ln\left[\frac{d(t)}{d(0)}\right] \qquad (5)$$

which describes the asymptotic rate of exponential divergence of two initially close trajectories where $d(t)$ is the distance between the two trajectories and

$d(t) = \|dx(t)\| + \|dy(t)\| + \|dP_x(t)\| + \|dP_y(t)\|$ in the 2-D case.

Usually, for real coordinates x and y and real momenta P_x and P_y, $\| \ \|$ is taken as the Euclidean distance. However, for complex coordinates and momenta we generalized it as the *norm* of the complex number (i.e. the distance in the complex plane). We calculated the Lyapunov exponent for both V_1 and V_2 in complex phase space to test its validity. It was found that for the real potential V_2, the calculated values of the Lyapunov exponent using the real phase space definition and the complex phase space definition are consistent with each other and they agree with the identification of the quasiperiodic and the chaotic regions made by using Poincare surfaces. Later in this section we identify the quasiperiodic and the chaotic regions of complex phase space for the complex potential V_1 by using the definition of Lyapunov exponents given in (5).

In order to obtain Poincare surfaces for the complex potential V_1, we solved Hamilton's equations in the complex plane. As in the case of the real potential, we collected the points (x, P_x) when $y = 0$ and (y, P_y) when $x = 0$ to obtain Poincare surfaces. Figures (13)-(16) show various projections of Poincare surfaces for different energies.

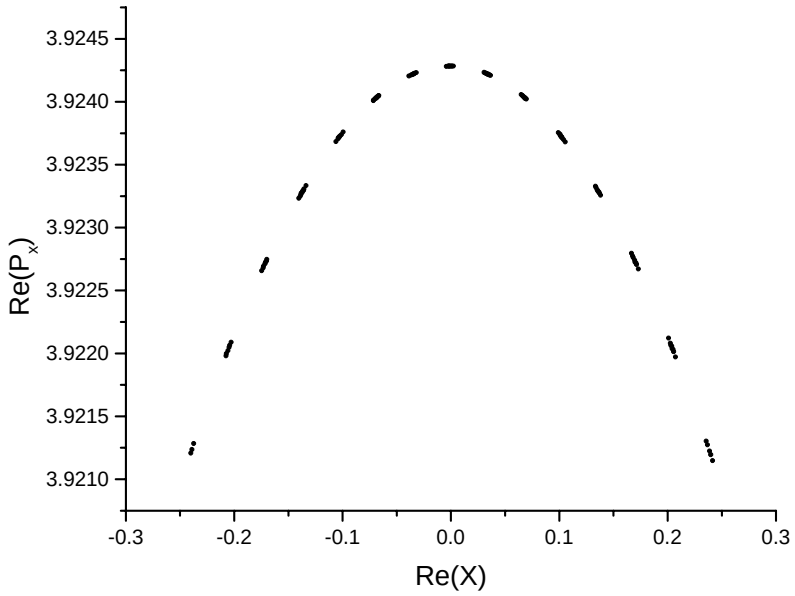

Fig. 13 Example of a Poincare surface of section at $y = 0$ of one trajectory of the complex potential V_1 in complex phase space for the energy $E = 6.0$, Only the real projections of the coordinate x and momentum P_x are shown here. Unlike for real potentials, curve is not closed. This energy corresponds to the regular motion.

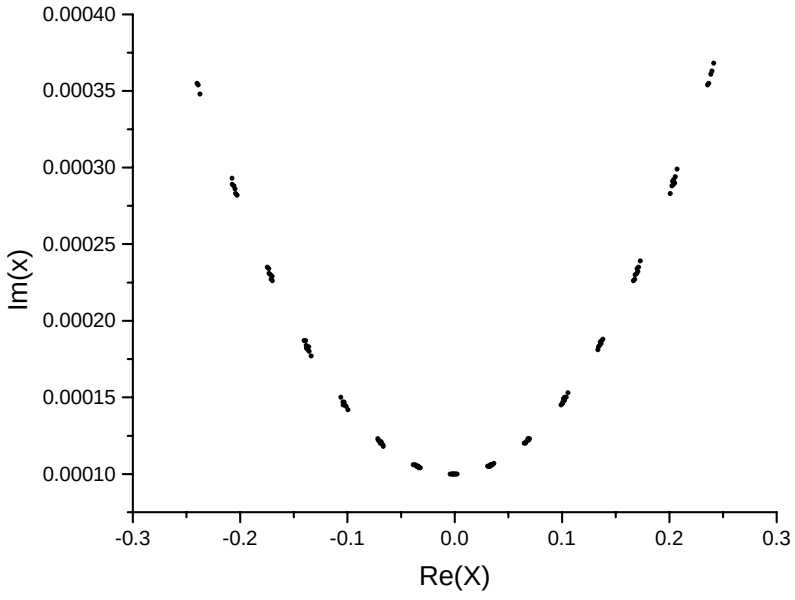

Fig. 14: Same as Figure 13. but only the projection of the Poincare surface of sections on the complex coordinate plane of x is shown here.

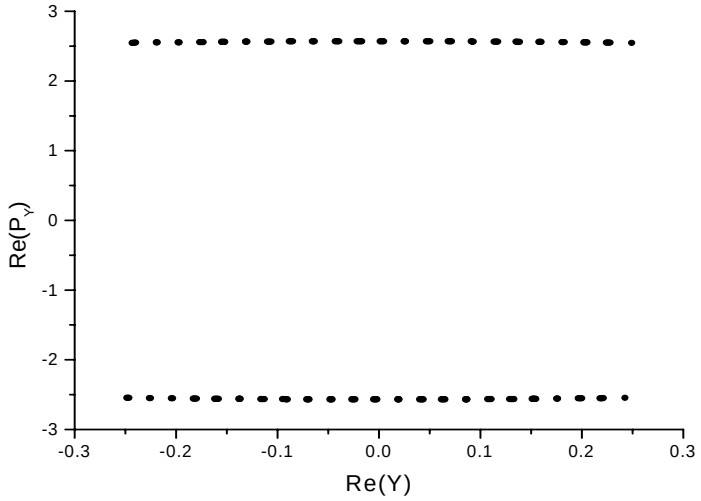

Fig. 15: Example of a Poincare surface of section at $x = 0$ of one trajectory of the complex potential V_1 in the complex phase space for the energy $E = 6.0$, Only the real projections of the coordinate y and momentum P_y are shown here. Unlike for real potentials, curves are straight lines, parallel to the real Y axis. For all energies less than 6.0, Poincare surfaces of section at $x = 0$ look similar to this when the motion is regular.

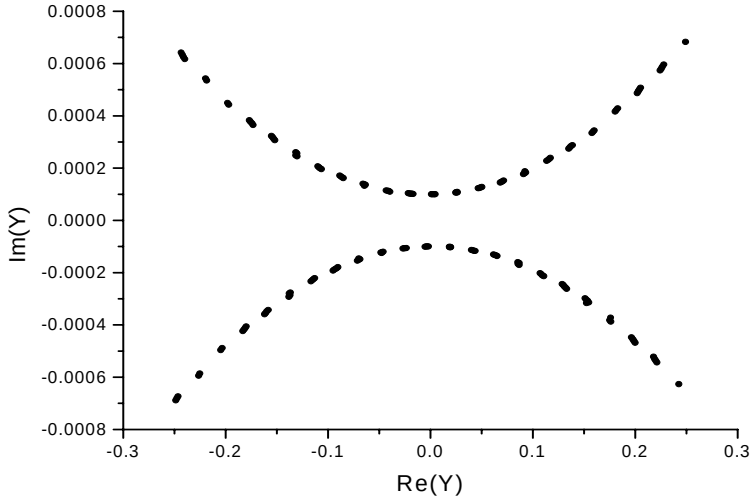

Fig. 16: Same as Figure 13. but only the projection of the Poincare surface of sections on the complex coordinate plane of y is shown here.

Figures (13) - (16) correspond to the quasiperiodic case while Figures (17)-(19) below correspond to mixed states of regular and ergodic motions.

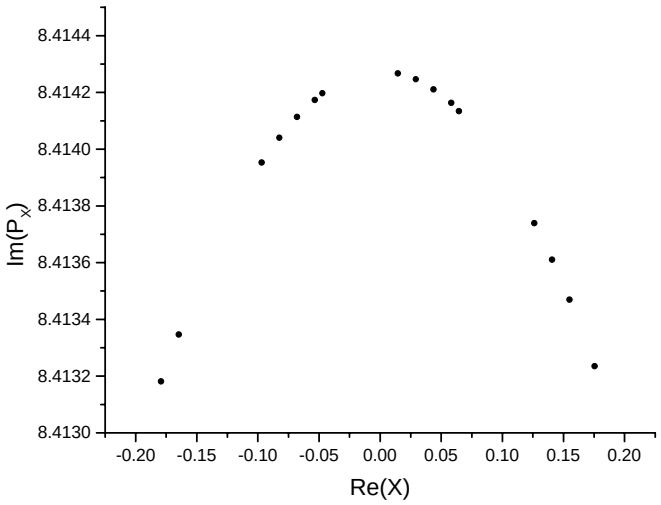

Figure 17: Example of a Poincare surface of section at $y = 0$ of one trajectory of the complex potential V_1 in the complex phase space for the energy $E = 59.0$, and the initial condition $f_x = 0.65$. Only the real projections of the coordinate x and momentum P_x are shown here. Energy E and f_x here corresponds to regular motion and the calculated Lyapunov exponent is negative. The Poincare surface corresponding to $x = 0$ looks similar to Figure 15.

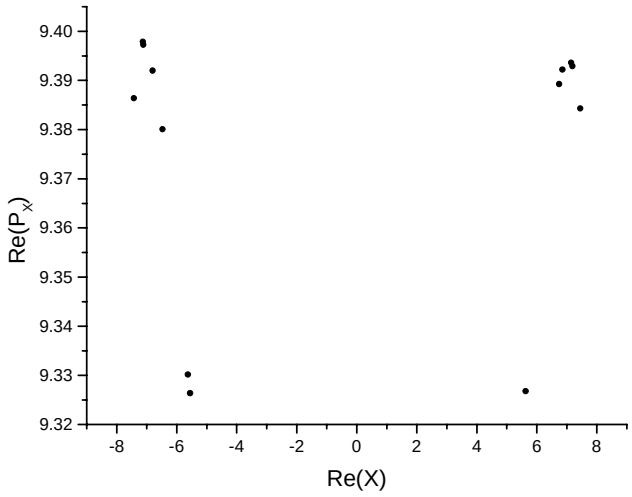

Fig. 18: Example of a Poincare surface of section at $y = 0$ of one trajectory of the complex potential V_1 in the complex phase space for the energy $E = 59.0$, and the initial condition $f_x = 0.7$. Only the real projections of the coordinate x and momentum P_x are shown here. Energy E and f_x here corresponds to chaotic motion and the Lyapunov exponent is now positive. The Poincare surface, obtained numerically, corresponding to $x = 0$ does not contain any points for these values of E and f_x.

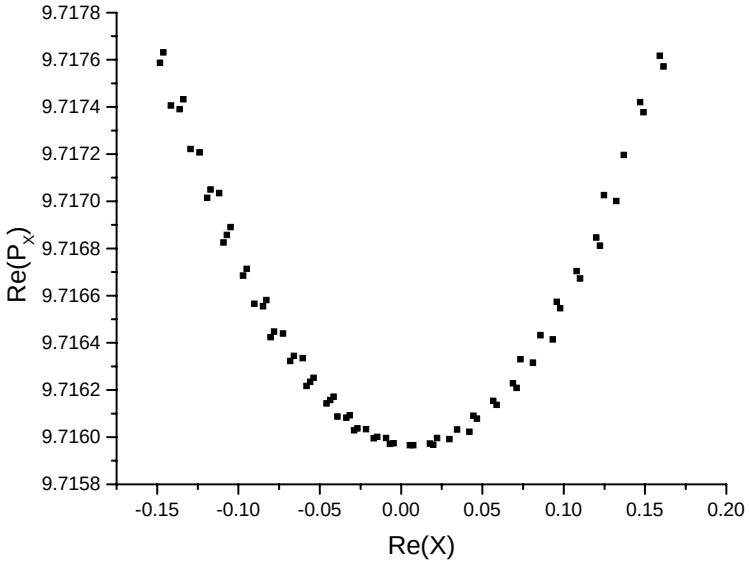

Fig. 19 Example of a Poincare surface of section at $y = 0$ of one trajectory of the complex potential V_1 in the complex phase space for the energy $E = 59.0$, and the initial condition $f_x = 0.75$. Only the real projections of the coordinate x and momentum P_x are shown here. Energy E and f_x here corresponds to regular motion and the Lyapunov exponent is negative. The Poincare surface corresponding to $x = 0$ looks similar to Figure 15.

It is evident from these figures that from the projections of Poincare surfaces, it is hard to distinguish between the quasiperiodic and ergodic regions. The main reason is that when the energy corresponds to chaotic regions, the number of points in the Poincare surfaces, generated numerically, are restricted to a very few or none. It appears as if the trajectories occupy the entire complex phase space when the motion becomes chaotic and the trajectory has to be monitored for a very long time to collect a sufficient number of points for the desired Poincare surface. This is not numerically feasible due to the generation of round off errors.

However, it is found that Lyapunov exponents based on (5) in the complex phase space can be used to identify both quasiperiodic and chaotic regions correctly. As an example, for $E = 59.0$ and $f_x = 0.68$ where $f_x = \dfrac{P^2{}_X}{P^2{}_X + P^2{}_Y}$ at $t = 0$, the Lyapunov exponent $L_e = -0.00018$. This corrsponds to regular motion and projection of the corresponding Poincare surface is shown in figure (17). However, when $E = 59.0$ and, $f_x = 0.7$, the Lyapunov exponent becomes $L_e = 0.000856$. This

corresponds to chaotic motion (Figure (18)). If we increase f_x further to the value 0.75 while keeping E fixed at 59.0, the motion becomes regular again giving the Lyapunov exponent $L_e = -0.00017$. We found that in most of the cases, when the Lyapunov exponent became positive, the Poincare surfaces did not have any points .

4. SEMICLASSICAL QUANTIZATION

When the system is quasiperiodic for real potentials, the semiclassical energy eigen values can be found by using Poincare surfaces [4]. The quantization conditions are

$$2\pi\left(n_1+\frac{1}{2}\right)\hbar = \oint_{C_x} p_x dx \qquad (y=0) \qquad (5)$$

$$2\pi\left(n_2+\frac{1}{2}\right)\hbar = \oint_{C_y} p_y dy \qquad (x=0) \qquad (6)$$

where curves C_x and C_y are closed curves in Poincare surfaces of sections $x=0$ and $y=0$ respectively. In [4], Noid and Marcus obtained the semiclassical energy eigen values for the potential V_2 for various values of the parameters in the potential and found that these values agree with the exact quantum mechanical eigen energies for the system.

In section 2. we saw that when the classical motion is quasiperiodic, the Poincare surfaces contain closed curves while when the motion becomes chaotic, these closed curves no longer exist. In this study, we extend the idea of Noid and Marcus to complex Poincare sections to obtain a quantization condition in the complex plane.

Instead of using the closed curves p_X vs x or p_Y vs y as in Figures (1) and (2) with the equations (5) and (6), we introduce the new quantization condition as

$$2\pi\left(n_1+\frac{1}{2}\right)\hbar = \int_{C_x} p_x dx \qquad (y=0) \qquad (7)$$

$$2\pi\left(n_2+\frac{1}{2}\right)\hbar = \int_{C_y} p_y dy \qquad (x=0) \qquad (8)$$

where now the curves C_x and C_y are closed contours in the projections of Poincare surface of sections $x=0$ and $y=0$ on the complex coordinate planes of x and y respectively and the integrals are now complex contour integrals rather than line integrals as the case in Noid & Marcus's work .

In this work, we calculated the semiclassical energy eigen values using both Noid and Marcus's method and our generalized method using contour integrals for the real potential V_2 and found out that both methods produce the same results up to the accuracy of the numerical methods used.

As it is evident from figures (13) - (16), in contrast to the closed curves obtained for a real potential, these projections of Poincare surfaces represent open curves with only a few points. As a result, the contour integral method or the Noid and Marcus's method cannot be directly applied for calculating semiclassical eigen energies for complex potentials. Alternative methods for obtaining semiclassical eigen energies are currently under investigation.

REFERENCES

[1] M.Henon and C.Heiles, Astron. J. 69, (1964) 73.
[2] D.W. Noid, M. L. Koszykowski, and R. A. Marcus, Ann. Rev. Phys. Chem. 32 (1981) 267 and references therein. K. S. Sorbie and N. C. Handy, Mol. Phy. 33 (1977) 1319.
[3] C.M.Bender, G.V.Dunne, P.N.Meisinger, M.Simsek, Phy. Lett. A, 311, (2001) 281.
[4] D.W. Noid and R. A. Marcus, J. Chem. Phy. 62 (1975) 2119. Randall B. Shirts and William P. Reinhardt, J. Chem. Phy. 77 (1982) 5204. Charles Jaffe and William P. Reinhardt, J. Chem. Phy. 77 (1982) 5191 and references therein.
[5] Asiri Nanayakkara, Sri Lankan Journal of Physics 1 (2000) 23.
[6] G. Contopoulos, L. Galgani and A. Giorgilli, Phy. Rev. A. 18, (1978) 1183. and F. Faisal and U. Schwengelbeck, Phy. Lett. A, 207 (1995) 31.
[7] W. H. Steeb and J. A. Louw, Chaos and Quantum Chaos, (World Scientific, 1986).